

MECHANICAL ALLOYING OF IRON-COATED NbC AND Si IN STIRRED MEDIA MILL

A. Al-Azzawi ^{a,*}, F. Kristály ^c, Á. Rácz ^b, P. Baumli ^a, K. Bohács ^b, G. Mucsi ^b

^{a*} University of Miskolc, Institute of Physical Metallurgy, Metal Forming and Nanotechnology, Miskolc, Hungary

^b University of Miskolc, Institute of Raw Material Preparation and Environmental Processing, Miskolc, Hungary

^c University of Miskolc, Institute of Mineralogy and Geology, Miskolc, Hungary

(Received 24 November 2018; accepted 08 February 2019)

Abstract

In the current research, the effect of mechanical alloying (MA) of iron-coated NbC and Si on the material's fineness and crystal structure was investigated. The MA experiments were carried out in a batch-type laboratory scale stirred media mill for various residence times up to 240 min in isopropanol. During MA, milling energy was measured, and stress energy (SE) was calculated. Morphology and material structural changes, during the mechanical alloying process, were determined by means of scanning electron microscopy (SEM) and powder X-ray diffraction (XRD), respectively. The particle size distribution of the product was measured by a Horiba 950 LA laser particle size analyser. Evolution of phases during high-energy milling of NbC, Al-Fe-carbide, Fe, and Si was studied as a function of specific milling energy. Transformations in the crystal structure were revealed, namely the generation of cementite and Nb-Si-carbide, which was proved by XRD results and thermodynamic calculations. As result of the experiments, optimum MA conditions were determined. The application of the mechanical alloying method gives the opportunity to produce nanocrystalline phase from the initial iron-coated NbC and Si powder.

Keywords: Niobium carbide; Silicon; Mechanical alloying; Nanostructure; Phase composition

1. Introduction

Efficient synthesis of materials with low energy demands is very important aspect for both scientific and industrial fields. It is in this area, mechanical alloying is very useful. MA is a solid state process which is employed in producing nanocomposite structures and compounds via a series of mechanochemical reactions [1-4]. The structure of the material gets disordered and defects are created [5] particularly when high energy ball mills like planetary mills or vibratory mills are used. These high energy mills change the surface properties of solid materials [6-8]. Mechanical alloying in wet media in tandem with ball mills is still highly unexplored area both in terms of fundamental research and technical research. The basic process involves elemental powders colliding with high speed stirred media, thus suffering plastic deformation leading to a high density of lattice defects and dislocations [9-11]. These effects in addition with momentary increase of temperature of

powders caught between the high speed balls will encourage the diffusion process. Homogenous alloy powders are produced as a result of all the above factors [12]. These nanocrystalline powders have a characteristic microstructure, mostly helpful in various potent applications [13, 14].

The present research aims at development of iron-coated NbC powder which has high wear resistance, hardness and thermal stability. These properties are tailor made for application areas of laser melt injection moulding, rapid tooling and laser assisted mould repair where NbC powder can be used as coatings [15]. Laser powder deposition is widely used in rapid tooling and for coating [16]. In situ [17] and ex situ [18-21] synthesis of Metal Matrix Composites have been reported using pre-prepared NbC by depositing (in situ) or MA method (ex situ) Nb-Si, Nb-Cr and Nb-Al composites. The iron-coated Niobium carbide was chosen for its ability to synthesise and formation of the Fe + NbC + Fe₃C composite with uniformly distributed nanocarbide

*Corresponding author: femali@uni-miskolc.hu



phases, which result in increasing the microhardness of the reinforcement powder [22]. This carbide exhibits some important characteristics for tribological applications additionally to high hardness [23]. However, fabrication of iron coated NbC has not been reported so far by MA.

Mixtures of iron coated NbC and Si powders corresponding to nominal composition of 85% NbC and 15% Si were characterised by X-Ray diffraction (XRD), scanning electron microscopy (SEM) and laser particle size analysis (LPSA). These techniques help in revealing the kinetics and mechanism of in situ formation of NbC during MA.

The aim is to report the possibility of in situ synthesis of nanocrystalline Si in NbC matrix (15wt% Si) with high energy ball mill at various times of 5, 15, 30, 60, 120 and 240 minutes. Investigating the properties of in situ iron coated NbC-Si composite as function of milling time and finally discussing the crystal structure transformations associated with NbC and Si. The changes are then compared to the raw materials of iron-coated NbC and Si prepared in laboratory using planetary mill.

2. Materials and methods

2.1. Scanning electron microscopy (SEM) and energy dispersive X-ray analysis

Scanning electron microscopy is a powerful tool appropriate for investigating composite materials' surfaces/cross-sections. The application of a low-energy electron beam in the analysis of materials at the nanoscale is playing a significant role in many research areas. It employs decelerated primary electrons for better resolution and specificity of the resulting analysis [24]. The type of SEM used to investigate the samples is an S-4800 Hitachi with Bruker YAG energy dispersive detector. The primary beam energy was 30 kV.

2.2. X-ray diffraction

The phase composition was determined by a Bruker D8 Advance XRD powder diffractometer (Cu-K α radiation, 40kV, 40mA) in parallel beam geometry (Göbel-mirror). Patterns were recorded in 2-70° (2 θ) range, with 0.007° (2 θ) steps in 42 seconds, with Vantec-1 position sensitive detector (1° window opening). Phase identification was made by Search/Match (multiple iterations) on ICDD PDF2-Release (2012).

2.3. Particle size analysis

Particle size distribution and geometrical specific surface area of the ground and mechanically alloyed material were measured and calculated by a Horiba

LA-950V2 laser particle size analyser in isopropanol media. Calculation of particle size distribution from measured data was carried out using the Mie theory, taking into account the refraction index of the material.

2.4. Materials

The raw materials used in this study are iron-coated niobium carbide and silicon. The iron-coated NbC used for laboratory experiments contains 53.04 wt% of Nb, 25.73 wt% of C, 19.74 wt% of Fe and 1.5 wt% of Al according to the scanning electron microscopy investigation as shown in Figure 1 and Table 1. The iron-coated NbC and Si were prepared in laboratory for mechanical alloying and it is discussed in detail below.

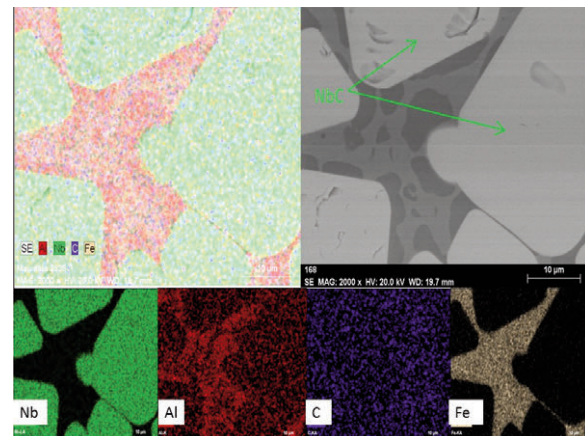


Figure 1. The scanning electron microscopy (mapping analysis) images of initial iron-coated NbC particles

Table 1. The chemical composition of NbC

Elements	C	Al	Nb	Fe	Total
wt %	25.73	1.5	53.04	19.74	100
At %	68.61	1.78	18.29	11.32	100

From the SEM images in Figure 1 it is possible to observe that the NbC particles are embedded in iron, which contains significant aluminium (Table 1) according to the X-maps. The X-ray diffraction analysis revealed the existence of Fe-Al-carbide and Fe as distinct phases, beyond NbC. Silicon sample was obtained from the Bay Zoltán Nonprofit Ltd. for Applied Research and its Industrial Laser Technology Laboratory in Budapest. Characteristic particle sizes of silicon after preparation were as follows: median particle size d_{50} = 7.18 μ m and 80% passing size d_{80} = 46.09 μ m.



2.5. Experimental

2.5.1 Material preparation in a planetary ball mill

The iron-coated NbC was prepared separately in a Retsch planetary ball mill prior to mechanical alloying in a stirred media mill. The aim of this step was to grind the feed iron-coated NbC down to finer than 63 μm size. The container of the mill was made of steel and filled with steel balls. The grinding ball size was 40 mm, and there were three of them in the mill chamber. After the first milling stage, the mill product was sieved at 63 μm, the fine size fraction was collected, and the coarse fraction was fed into the mill again and ground until reaching finer size than 63 μm (quantitatively ground). The scanning electron microscopy images of the iron-coated NbC powder after the grinding process can be seen in Figure 2.

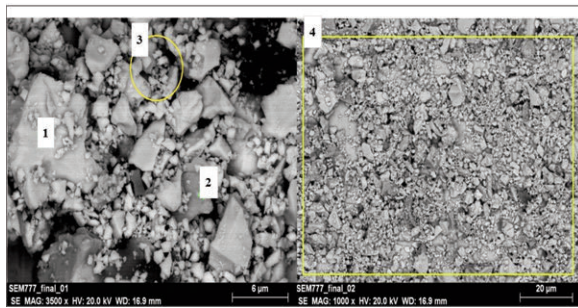


Figure 2. SEM images of the iron-coated NbC powder after the grinding process

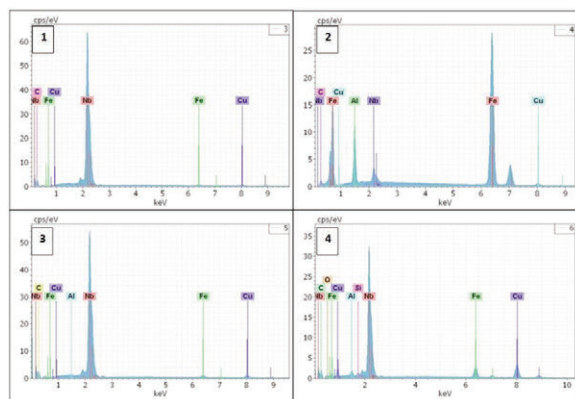


Figure 3. EDS spectrum of SEM images in Fig. 2.

From the EDS spectrum analysis of point 2 (in Figure 3) of SEM images in Figure 2, Fe-Al-carbide particles are observed covering the NbC particles, which have been detached from between NbC particles during the milling process. Also, it can be observed that there are some signs of copper in EDS analysis, because the powder was placed on the top of a copper tape as a conductive layer for the SEM and EDS analysis.

The Silicon was prepared separately for mechanical alloying with the same planetary ball mill. The aim was to grind the feed silicon down to finer than 63 μm. The grinding process and circumstances were similar to that of the previously presented case.

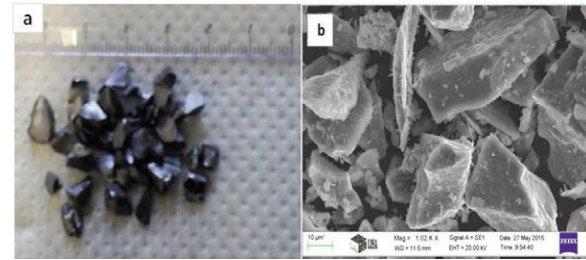


Figure 4. Photo and SEM images of silicon powder (a) before grinding (b) after the grinding process

Images of the silicon powder before and after the grinding are shown in Figure 4. The effect of the grinding process on the particle size is observed, which is reduced from the initial 5 mm down to ≤ 63 μm. Furthermore, the shape of the particles became irregular, with sharp edges compared to the original rounded particles.

2.5.2 Mechanical alloying

The previously prepared (milled and sieved) iron-coated NbC and silicon samples were mechanically alloyed in a batch stirred media mill with a grinding chamber volume of 530 cm³. The grinding chamber was equipped with water jacket cooling in order to control the temperature of the grinding chamber. During the mechanical alloying experiments, the temperature of the grinding chamber was a constant 30±2 °C. The stirrer consisted of perforated triangular shaped disc rotors fixed on a drive shaft. The revolution number (circumferential speed of the rotor) can be adjusted by a frequency control unit. The consumed electric power during the experiments was measured by a microcomputer-controlled digital energy meter Carlo Gavazzi WM1-DIN for the characterization of the specific grinding energy. The energy meter recorded the electric work in cumulated form; in this way, the grinding work could be calculated as the difference between the initial and the final values. By measuring the no-load electric power consumption, the instantaneous power, and the mass of the product, the specific milling work can be determined as follows:

$$W_s = \frac{\int (P(t)) dt}{m_p} \tag{1}$$

where P(t) is the measured electric instantaneous



power and m_p is the mass of the final product. The milling experiments were carried out in a stirred ball mill using different milling times: 5, 15, 30, 60, 120 and 240 minutes. The circumferential speed (tip speed) of the rotor in the stirred ball mill was 10.56 ms^{-1} . The weight of the feed material was iron-coated NbC 24.6 g and Si 4.35 g with 147.36 g isopropanol added as the liquid medium for one batch. The media filling ratio was 70% during MA. The grinding medium was sintered zirconium silicate beads with the size range of 1.0-1.2 mm, specific weight of 4.1 kg/l and microhardness was 1000 HV.

3. Results and discussion

3.1 Material fineness

Figure 5 shows the change of the volume ratio as function of changing particle size in the mechanically alloyed iron-coated NbC+Si particles.

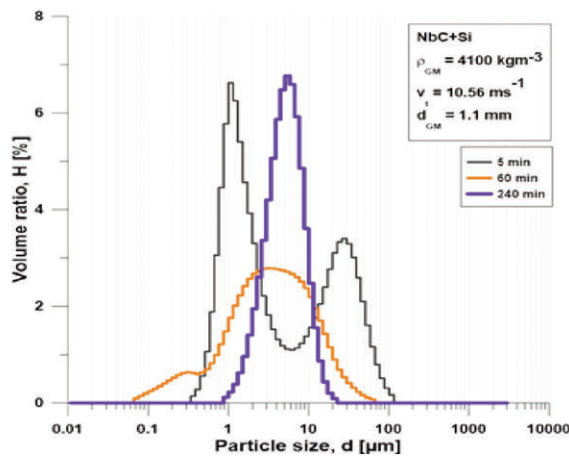


Figure 5. Volume ratio of the mechanically alloyed iron-coated NbC+Si

From Figure 5, it can be stated that the shape of the curve is bimodal in the initial stages of experiment and it changes with residence time. After 60 min residence time, the curve can be observed as shifted from bimodal to a unimodal shape, dominantly unimodal, and the particle size range also changes as function of time. The narrowest particles were produced after 240 min.

Figure 6 shows the cumulative particle size distribution curves of the mechanically alloyed NbC+Si particles. Significant fluctuation can be observed in the particle size distribution. Remarkably coarsening of the particles appears at 30 min residence time, probably due to the aggregation and/or agglomeration and/or mechanical alloying of the particles. After this, the NiC+Si ground material became finer, coarser and, then, finer again. No significant shift in particle size either progressive or

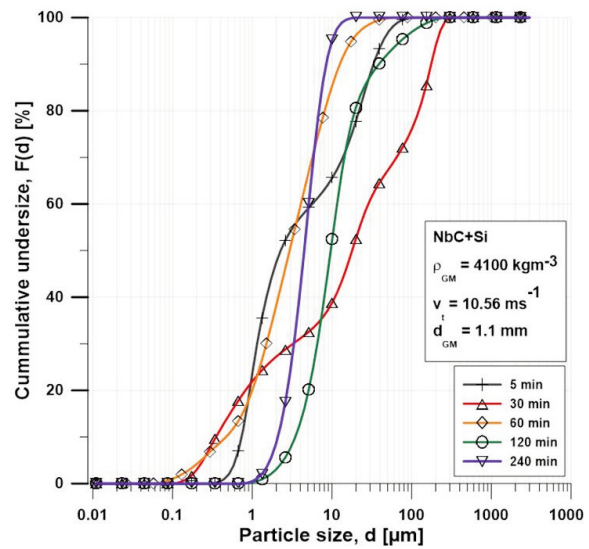


Figure 6. Cumulative particle size distribution curves of the mechanically alloyed iron-coated NbC+Si

regressive was observed. However, this shift was to be expected as in the case of brittle materials in general. But, when the grinding kinetics was investigated, the non-brittle behaviour of the materials was found to be cause behind this behaviour which results in more deformation and structural changing than particle size reduction.

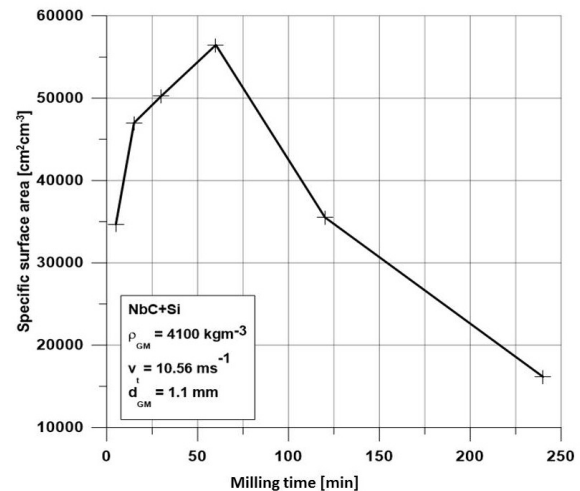


Figure 7. The specific surface area as a function of milling time

In Figure 7, the geometric (outer) specific surface area is plotted as a function of milling time. A sudden decrease in specific surface area was noticed at 60 min milling time in the stirred media mill. According to the kinetic consideration in the milling procedure, it can be divided into three main stages. In the first stage, the specific surface area rises linearly with the milling time (the so-called Rittinger section) with the

maximum specific surface area reached ($56\,459\text{ cm}^2\text{cm}^{-3}$) at 60 min milling time. In the second stage, the slope of the specific surface area decreases (section of aggregation), while in the third stage, the specific surface area decreases drastically with the milling time (which can be explained by the phenomenon of agglomeration) down to $16\,000\text{ cm}^2\text{cm}^{-3}$. However, from the cumulative undersize curves, no tendency can be observed; the specific surface are calculated from it shows the general trend [25] that was to be expected with brittle materials.

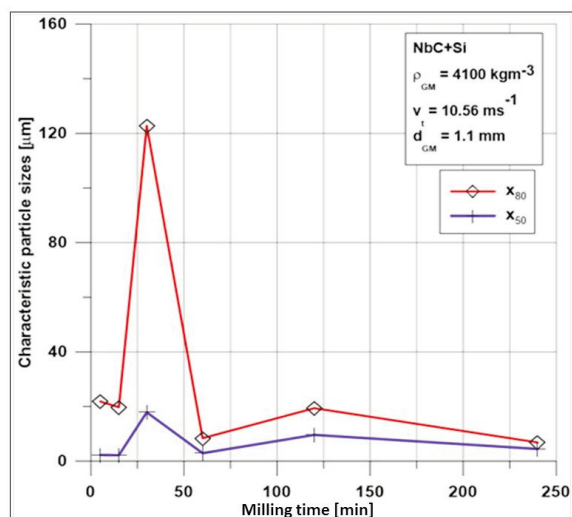


Figure 8. Characteristic particle sizes (d_{50} and d_{80}) as a function of milling time

Figure 8 shows the variation of the characteristic particles size values as a function of milling time for (NbC+Si) powder mixture, specifically with the median and 80% passing size plots. It is evident that the maximum particle size of the starting powder mixture was about $63\text{ }\mu\text{m}$. Comparing with the growing trend depicted by diameter on cumulative d_{50} , the median particle size of (NbC+Si) powder mixture in diameter and d_{80} reaches a maximum at 30 min milling time and then stabilizes between 60 and 240 min. However, during this process, the primary niobium carbide and silicon particles suffer from phenomenon of cold welding following the work hardening, resulting in the activation of the fracture mechanism. When the rate of cold welding and fracturing processes reach equilibrium, the steady state is achieved as reported by Zhang et al. [26].

3.2 Microstructure

The samples for SEM analysis are prepared by taking a small amount of (NbC+Si) powder after each milling process at 5, 15, 30, 60, 120 and 240 min, then the powder is placed in the resin mould. After the resin dries, the particles of powder were on the upper

surface of the sample and ready for SEM investigation.

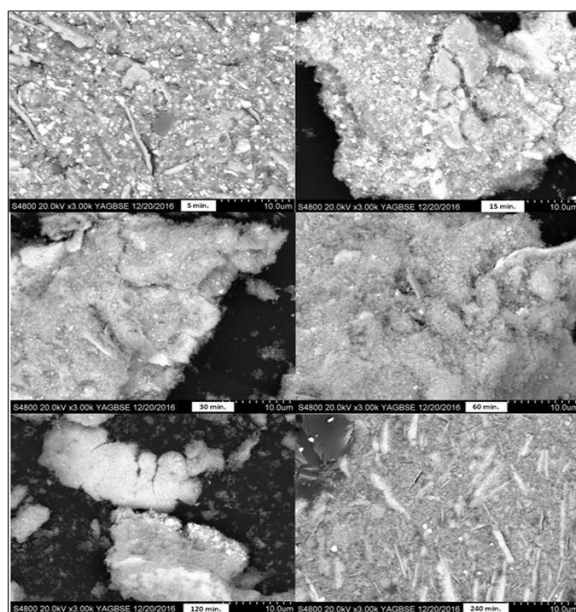


Figure 9. SEM images of the iron-coated NbC-Si powder after mechanical activation for 5-240 min milling time

From the SEM images in Figure 9, the effect of milling for different periods of time (5-240 min) on the variation of the particles size of NbC-Si powder can be seen. At the beginning at 5 min milling time, the particle size starts to decrease, then the agglomeration stage can be noticed at longer milling periods (240 min). It is not possible to distinguish particles of NbC from Si, which indicates that they have reached the nanometer size.

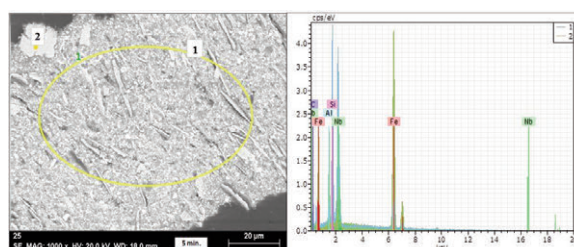


Figure 10. SEM images and EDS spectrum of the iron-coated NbC-Si powder after MA for 5 min milling time

Figures 10 and 11 show the SEM images and EDS spectrum of the NbC-Si-Fe-Al alloys after 5 and 240 min of the process, respectively, where the effect of milling can be seen for different times, namely the microstructure of the NbC-Si powder and the particle size. It is known that the MA process consists of three main stages: cold welding, fracturing, and steady-state condition [27]. Due to the high surface energy of the

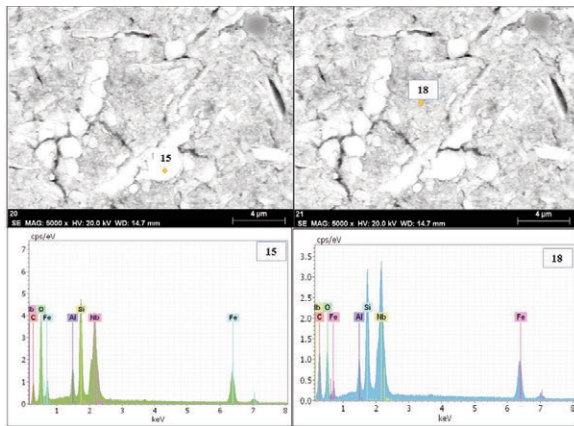


Figure 11. SEM images and EDS spectrum of the iron-coated NbC-Si powder after MA for 240 min milling time

fine particles and the consequent domination of cold welding and agglomeration over fracturing mechanisms, irregularly shaped powders with a wide particle size distribution are developed at the early stages of milling (e.g. 5 min).

By increasing the milling time, the powder particles are hardened, and due to the accumulation of strain energy [28], the particle hardness increases, and therefore the tendency of cold-welded powders to fracture increases, and the particle size is significantly reduced. Afterward, a balance between the cold welding and fracturing rates is achieved, and the particle size reaches its steady-state condition [28, 29], which is associated with the narrow particle size increasing as it is shown in Figure 11.

The SEM image in Figure 11 shows that at low milling time (e.g. 5 min), the element distribution is uniform, and the EDS spectrum image clearly presents a homogeneous element distribution. Also, at sufficiently high milling time (e.g. 240 min), the element distribution is more uniform, and that the difference between dark and light areas is the result of little difference in the concentration of the carbon element, thereby indicating a sufficient milling time for alloying.

3.3 Phase composition

Figure 12 shows the XRD spectra of the iron-coated NbC-Si milled powders as a function of milling time. As can be seen from the patterns, in the initial powder mixture, sharp diffraction peaks related to NbC, Si and Fe are evident. Also, minor phases such as Al-Fe-carbide and Fe-carbides are observed. At the initiation of milling, due to the development of nano-sized structure and the introduction of a high level of micro-strain, the sharp peaks are considerably broadened. By further milling, the peaks of the initial materials gradually vanish.

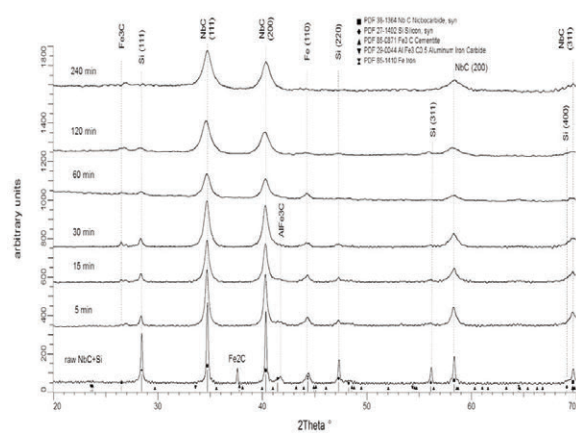


Figure 12. XRD images of iron-coated NbC-Si powder after MA for different milling times

The further analysis of the XRD patterns indicates that increasing the milling time has a significant effect on the transformation of different phases in the powders. The peak broadening caused by crystallite size reduction is observed for each phase, with the Si being significantly reduced already at the 5 min stage. After 240 min of milling, it was observed that the diffraction peak of silicon has disappeared, meaning the silicon changed to an amorphous phase. Since the formation of the amorphous phase during MA depends on several factors such as the milling conditions and the alloying system, different amorphisation reactions have been proposed [30]. The one consisting of a shift in the peak position and a continuous broadening of the XRD peaks due to a continuous reduction of the effective crystallite size is responsible for amorphisation of the present alloying system during MA. The XRD peaks have revealed that the NbC(111) and NbC(200) phase powder mixtures exhibit a series of changes during the milling. Compared to the starting material, the NbC phase demonstrates lower and broader diffraction peaks with the net height and net area increasing with the milling time until reaching the maximum value at 30 min of milling time, then decreasing until reaching the minimum value at 60 min, and then increasing again after 120 min of milling time. This phenomenon demonstrates that the powder mixture only undergoes sub-microstructural changes of NbC phase owing to the severe plastic deformation of the Nb particles [31, 32].

Stirred media milling for 240 min or more leads to a remarkable broadening of Nb diffraction peaks and a decrease in the intensity of Si and Fe diffraction peaks. The peaks of Si and Fe disappear after 120 min of milling, indicating the formation of a solid solution (or secondary solid solution) of Si, C and Fe phase in NbC phase. It is well known that high velocity stirred media milling supplements an input of high energy to the powder system. During this process, a large

number of flaws, including dislocations and new grain boundary, are generated, rendering the diffusion between different components facile and the occurrence of a solid solution of Si and Fe phase in NbC phase.

Stirred media milling provides the particles an intense plastic deformation at extremely high strain rate, which results in the creation of high-density lattice defects and dislocations, as well as the recovery phenomena [11, 33]. When the rate of the former is higher, the dislocations increase, resulting in a dislocation cell structure that ultimately creates low-angle grain boundaries. As the milling continues, low-angle grain boundaries transform into a whole nanocrystalline structure. In this stage, the crystallite size decreases and the lattice strain increases dramatically. The constant values of crystallite size and lattice strain reveal the balance of the creation and disappearance of dislocations.

4. Summary

An ultrafine nanocrystalline Nb-Si-Fe-C alloy powder is produced by green chemistry in stirred media milling at room temperature. During this process, the particles undergo cold welding, plastic deformation and work hardening and recovery stages. Milling time is an influencing parameter in producing alloy powders. As the velocity reaches up to 10.56 ms⁻¹, cold welding is the dominant mechanism during milling, and no solid solution has been observed even after milling for 240 min. The ideal milling conditions are 10.56 ms⁻¹ for 240 min, leading to nanocrystalline Nb-C-Fe and Si alloy powder particles with a crystallite size under 20 nm.

Acknowledgements

We would like to thank Janos Csizmazia, Dr Maria Sveda, Mrs Aniko Markus, Mrs Napsugar Nyari Bodnar, for their assistance to complete this research work. Special thanks to Prof. Dr George Kaptay for his insightful comments and suggestions during the preparation of this paper. The described article was carried out as part of the GINOP-2.3.2-15-2016-00027 "Sustainable operation of the workshop of excellence for the research and development of crystalline and amorphous nanostructured materials" project implemented in the framework of the Szechenyi 2020 program. The realization of this project is supported by the European Union.

References

- [1] M. Krasnowski, T. Kulik. J. Intermetallics, 18 (2010) 47–50.
- [2] M.M. Verdian. J. Mater. Manuf. Processes, 25 (2010) 1437–1439.
- [3] R. Yazdi, S.F. Kashani, Int. J. Modern Phys, 5 (2012) 581–588.
- [4] T.T. Sasaki, T. Ohkubo, K. Hono. J. Acta Mater. 57 (2009) 3529–3538.
- [5] P. Balaz, M. Achimovicová. J. Hydrometallurgy, 84 (2006) 60–68.
- [6] P. Baláz, Extractive metallurgy of activated minerals, Elsevier, Amsterdam, 1st, 10 (2000) p. 81–93.
- [7] É. Kristóf-Makó, A.Z. Juhász. J. Thermochim.Acta, 342 (1999) 105–114.
- [8] K. Tkáčová, Mechanical activation of minerals, Elsevier, Amsterdam, (1989)p. 293.
- [9] A. Mostaed, E. Mostaed, A. Shokuhfar, H. Saghafian, H.R. Rezaie, J. Defect and Diffus Forum, 283(2009) 494–498.
- [10] E. Hellstern, H.J. Fecht, Z. Fu, W.L. Johnson, J. Appl Phys, 65 (1989) 305–310.
- [11] C.C. Koch, J. Nanostruct Mater, 2 (1993) 109–129.
- [12] M.H. Enayati, G.R. Aryanpour, A. Ebnonnasir, Int. J. Refract Metals Hard Mater, 27 (2009) 159–163.
- [13] B.B. Panigrahi, J Mater Sci Eng A, 460 (2007) 7–13.
- [14] D. Janovszky, F. Kristaly, T. Miko, M. Sveda, A. Sycheva. J. Min. Metall. Sect. B-Metall. 54 (3) B (2018) 349 - 360.
- [15] J. Mazumder, A. Schifferer, J. Choi. J. Mater. Res. Innovations, 3 (1999) 118–131.
- [16] R. Vilar. J. Laser Application, 11(1999) 64–79.
- [17] R. Colac,o, R. Vilar. J. Laser Application, 15(2003) 267–272.
- [18] J.C. Lima, A.R. Jerônimo, A. Gomez, S.M. Souza, D.M. Trichês, C.E.M. Campos, T.A. Grandi, S. Kycia, J. Non-Cryst Solids, 354 (2008) 4598–4602.
- [19] J.C. Lima, T.O. Almeida, A.R. Jerônimo, S.M. Souza, C.E.M. Campos, T.A. Grandi, J. Non-Cryst Solids, 352 (2009) 109–115.
- [20] Rock C, Qiu J, Okazaki K. J. Mater Sci, 33 (1998) 241–246.
- [21] X.L. Wang, K.F. Zhang, J. Alloys Compd, 490 (2010) 677–683.
- [22] K.A. Yazovskikh, S.F. Lomayeva: J. Alloys and Compounds.586 (2014) 65–S67.
- [23] M. Skopp, A. Woydt, I. Dörfel, K. Wittke, J Wear. 218 (1999) 84–9.
- [24] T.L. Kirk. J. Advances in imaging and electron Physics, 204 (2017) 39–109.
- [25] A.Z. Juhász, L. Opoczky. Mechanochemistry and agglomeration, Building material, 55-3, Silicon Science Scientific Association (in Hungarian), Budapest, (2003) p. 86–90
- [26] D.Z. Zhang, M.L. Qin, Rafi-ud-din, L. Zhang, X.H. Qu. Int. J. Refractory Metals and Hard Materials, 32 (2012) 45–50.
- [27] D.R. Maurice, T.H. Courtney. J. Metallurgical Transactions A, 21 (1990) 289–303.
- [28] C. Suryanarayana, T. Klassen, E. Ivanov, J. Mater Sci, 49(19) (2011) 6301–6315.
- [29] L. Lu, M.O. Lai. J. Mater Des, 16 (1995) 33–39.
- [30] Weeber AW, Bakker H. J. Physica B: Condensed Matter, 135 (1988) 93–135.
- [31] S.S. Razavi Tousi, R. Yazdani Rad, E. Salahi, I.



- Mobasherpour, M. Razavi. J. Powder Technol, 192 (2009) 346–351.
- [32] J.B. Fogagnolo, M.H. Robert, E.M. Ruiz-Navas, J.M. Torralba. J. Mater Sci, 39 (2004) 127–132
- [33] M.H. Enayati, G.R. Aryanpour, A. Ebnonnasir. Int J. Refract Metals Hard Mater 27 (2009) 159–163.

MEHANIČKO LEGIRANJE PRAHA NbC I Si PREVUČENOG GVOŽĐEM U MLINU SA OBRTNIM KUĆIŠTEM

A. Al-Azzawi ^{a,*}, F. Kristály ^c, Á. Rácz ^b, P. Baumli ^a, K. Bohács ^b, G. Mucsi ^b

^{a*} Univerzitet u Miškolcu, Institut za fizičku metalurgiju, oblikovanje metala i nanotehnologiju, Miškolc, Mađarska

^b Univerzitet u Miškolcu, Institut za pripremu sirovina i zaštitu životne sredine, Miškolc, Mađarska

^c Univerzitet u Miškolcu, Institut za minerologiju i geologiju, Miškolc, Mađarska

Apstrakt

Tokom ovog istraživanja ispitivan je uticaj mehaničkog legiranja praha NbC i Si prevučenog gvožđem na finoću materijala, kao i na njegovu kristalnu strukturu. Eksperiment mehaničkog legiranja je izveden u mlinu sa obrtnim kućištem u laboratorijskim uslovima, tokom različitih vremenskih perioda do 240 minuta i u prisustvu izopropanola. Tokom mehaničkog legiranja izračunata je energija mlevenja, kao i energija napona. Morfologija i strukturne promene u materijalu tokom ovog postupka su određene pomoću skenirajućeg elektronskog mikroskopa (SEM), kao i rengentskom difrakcijom (XRD) praha. Raspodela čestica različitih veličina je izmerena pomoću lasera za analizu veličine čestica Horiba 950 LA. Razvoj faza tokom dinamičnog mlevenja NbC, Al-Fe-karbida, Fe i Si je ispitivan kao funkcija specifične energije mlevenja. Otkrivene su promene u kristalnoj strukturi, odnosno formiranje cementita i Nb-Si- karbida, što je i dokazano XRD analizom i termodinamičkim izračunavanjima. Kao rezultat eksperimenata, utvrđeni su optimalni uslovi za mehaničko legiranje. Primena metode mehaničkog legiranja pruža priliku da se dobije nanokristalna faza od početnog praha NbC i Si prevučenog gvožđem.

Ključne reči: Niobijum karbid; Silicijum; Mehaničko legiranje; Nanostruktura; Sastav faza.

